2022

CANCER AND QUIESCENCE: INVESTIGATING HOW THE DREAM COMPLEX AND RETINOBLASTOMA REGULATE THE CELL CYCLE

Lydia Rotman
Michigan Technological University, larotman@mtu.edu

CANCER AND QUIESCENCE: INVESTIGATING HOW THE DREAM COMPLEX AND RETINOBLASTOMA REGULATE THE CELL CYCLE

By

Lydia A. Rotman

A THESIS

Submitted in partial fulfillment of the requirements for the degree of

MASTER OF SCIENCE

In Biological Sciences

MICHIGAN TECHNOLOGICAL UNIVERSITY

2022

This thesis has been approved in partial fulfillment of the requirements for the Degree of MASTER OF SCIENCE in Biological Sciences.

Department of Biological Sciences

Thesis Advisor:	*Dr. Paul Goetsch*
Committee Member:	*Dr. Thomas Werner*
Committee Member:	*Dr. Stephen Techtmann*
Department Chair:	*Chandrashekhar P. Joshi*

Table of Contents

List of Figures

Author Contribution Statement

For this project, I worked collaboratively with Karl Schneider, who was responsible for the majority of the tissue culture work and helped extensively with the Flow Cytometry experiments. Samantha Siefert and I worked together to establish and complete the Western blot experiments. For help with the experiments, Akayla Weatherby, Samantha Siefert, and Karl Schneider were vital for this project.

Acknowledgements

A big thank you to Karl Schneider, Samantha Siefert, and Akayla Weatherby for their assistance in the lab. I could not have done this without you all.

An even bigger thank you to Professor Goetsch for guiding me through a year of learning and practicing.

Definitions

Quiescence - A cellular state of inactivity or dormancy

Proliferation - Cell growth and division

List of Abbreviations

CDK - Cyclin Dependent Kinase

ChIP - Chromatin Immunoprecipitation

DNA - Deoxyribose Nucleic Acid

DREAM complex - Dimerization partner, RB-like, E2F and multi-vulval class B. A protein complex assembled by p130 that represses gene transcription.

HFF - Human Foreskin Fibroblasts

kDa - kilodaltons, a measure of protein weight.

OVCAR3 - Epithelial cells that were isolated in 1982 from the malignant ascites of a patient with progressive adenocarcinoma of the ovary.

PAR - Palbociclib, abemaciclib, and ribociclib drug cocktail

PBS - Phosphate Buffered Saline

PP1 - LOOK UP

pRb - Retinoblastoma protein

R point - Restriction Point

RCF - Relative Centrifugal Force

RNA - Ribose Nucleic Acid

RPM - Rotations Per Minute

SKOV3 - An ovarian cancer cell line derived from the ascites of a 64-year-old Caucasian female with an ovarian serous cystadenocarcinoma.

Abstract

An estimated 1.9 million people in the United States will be diagnosed with cancer in 2022. Cancer is characterized by uncontrolled cell growth, resulting from loss-of-function of key cell cycle regulatory proteins. The retinoblastoma protein (pRb) and p130, are two proteins that regulate cellular entry into the cell cycle. Both pRb and p130 repress expression of cell cycle genes, with pRb interacting with and suppressing E2F-DP transcriptional activators and p130 assembling in the DREAM transcriptional repressor complex. When normal cells receive signals to enter the cell cycle, cyclin and cyclin-dependent kinase (CDK) complexes phosphorylate pRb and p130, causing both to release from their respective complexes. Recently, CDK inhibitors have been proven to be effective chemotherapeutics, as they effectively lock pRb and p130 in their cell cycle repressive functions. Unfortunately, many ovarian tumors remain resistant to CDK inhibitor treatment. However, to date, no study has systematically evaluated how ovarian cancer affects both pRb and p130 function. Using flow cytometry, we confirmed that the SKOV3 ovarian cancer cell line responds to CDK inhibition but the OVCAR3 ovarian cancer cell line does not respond to CDK inhibition. Using western blot and expression analysis, we evaluated pRb and p130 response to CDK inhibition in SKOV3 cells, as compared to normal human foreskin fibroblasts (HFFs). We observed that although both pRb and p130 protein remain similarly expressed throughout the cell cycle, repression of 2 cell cycle genes, CCNB2 and MCM5, in CDK inhibited cells appears to be perturbed in the SKOV3 cell line, as compared to HFF cells. This study will lay the groundwork for future studies aimed to differentiate whether pRb or p130 dysfunction is causing the cell cycle gene dysregulation we observed in the SKOV3 cell line.

Key Points

- Comparing DREAM and pRb in quiescent vs. non-quiescent cancerous and noncancerous cell lines can help discern specific points of deregulation in the quiescence to proliferation pathway.
- The DREAM complex is a multiprotein complex that is assembled by p130. p130 binds E2F repressors and their DP binding partner to the MUVB core, allowing for transcriptional repression of the cell cycle by binding to DNA promoters.
- Protein retinoblastoma regulates cell cycle gene transcription by binding and suppressing E2F transcription activators, preventing them from initiating gene transcription.
- Cyclin/CDK complexes regulate cell proliferation by phosphorylating p130 and pRb, which inactivates the proteins. Once these proteins are inactivated, cell cycle genes can be transcribed, allowing the cell to enter the S phase.
- Cancer arises when cells begin to divide uncontrollably. When the DREAM complex and pRb become mutated, the cell loses its ability to stop proliferation when signaled by outside stimuli. However, some cancer cells can still enter quiescence if DREAM or pRb are still functioning.

1 Introduction

The cell cycle is a highly complex system that is closely regulated by the Retinoblastoma protein (pRb) and p130.[1] pRb and p130 are tumor suppressor proteins that suppress cell cycle gene transcription, which prevents a cell from entering the cell cycle. When a cell doesn't need to divide, p130 suppresses the cell cycle by binding E2F regressors to the promoter region of cell cycle genes.[2-4] Unlike pRb, p130 binds to the 5-subunit MuvB core subcomplex to form the DREAM complex that can bind repressors to the promoters of genes (Figure 1).[5-7] pRb suppresses cell cycle gene expression by binding and inhibiting E2F activators on gene promoters (Figure 2). Both p130 and pRb are regulated by Cyclin D and cyclin-dependent kinases (CDKs) 4/6. If a cell needs to re-enter cell division, Cyclin D works in conjunction with CDK4/6 to phosphorylate pRb and p130 to dissociate them from the DNA and halt their repression of the target cell cycle genes (Figure 2).[8] When cells don't need to divide for extended periods, pRb and p130 suppress cell cycle genes, and cells enter quiescence, also known as G0.[5,9]

Quiescence is defined as a reversible non-proliferative state that is completely separate from the cell cycle.[10,11] Quiescence allows cells to maintain a specific number of cells in a tissue, which is vital for organismal health. Due to experimental design in the early 20th century, the cell cycle became widely studied, and far fewer studies were conducted on quiescent cells.[11] In contrast to normal cells, cancer cells typically replicate continuously and independently from extracellular signals. While unchecked cell growth is a hallmark of cancer, some cancer cells retain their ability to quiesce. This indicates that either pRb or p130 is present and has retained some function. Current cancer therapies target the mitotic spindles and microtubules of dividing cells. Quiescent cancer

cells can lay dormant during chemotherapy and radiation, allowing them to survive treatment.[12] They can remain dormant for years after treatments are completed, resulting in recurrent and metastatic cancer. Currently, there is a great understanding of how pRb and p130 function in noncancerous cells, but there is a lack of knowledge of how they function in cancer cells that can quiesce compared to cancer cells that cannot quiesce. By understanding what causes cancer cells to quiesce, we can more effectively treat cancer in the future.

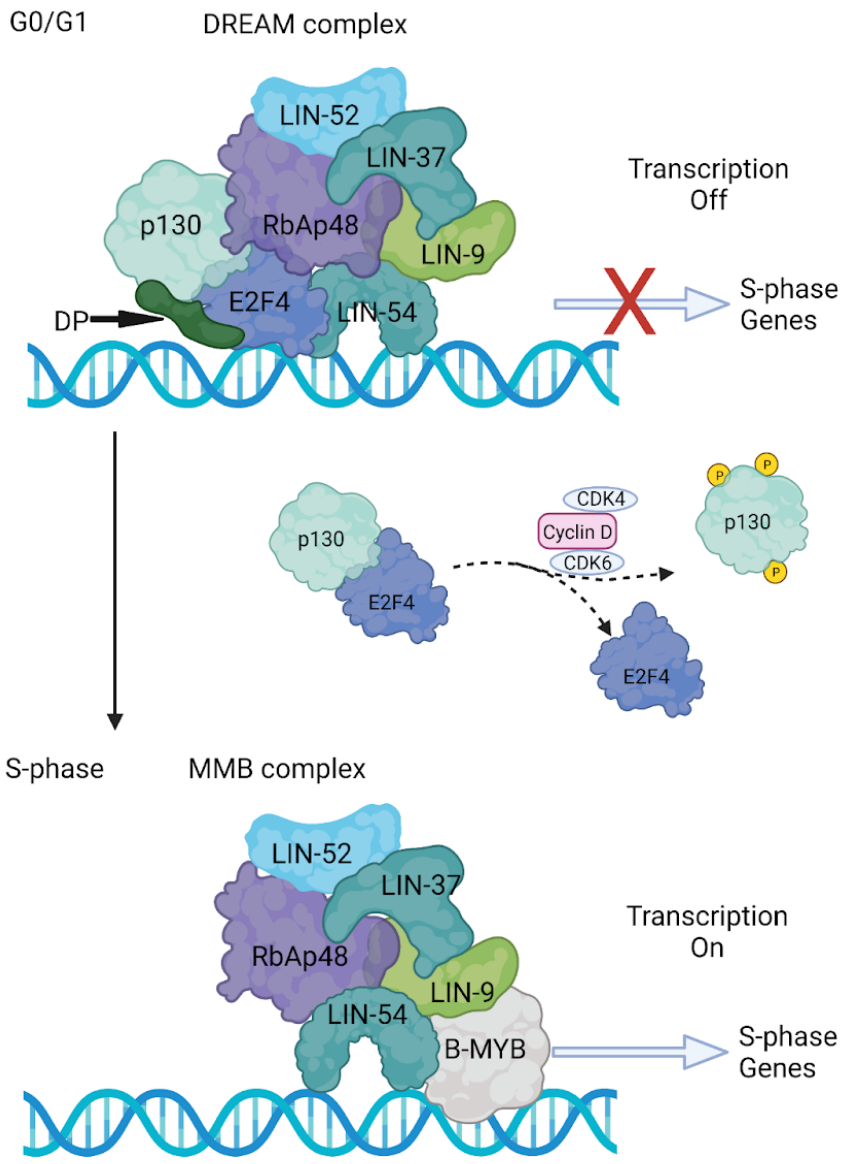

Figure 1: The top image visualizes the MuvB core as the DREAM complex when bound to p130 repressing transcription during the G0 and G1 phases. The bottom half depicts the MuvB core interacting with B-Myb to form the MMB complex, activating transcription. This image is based on an image from (Rashid, Yusof, and Watson, 2011).[13]

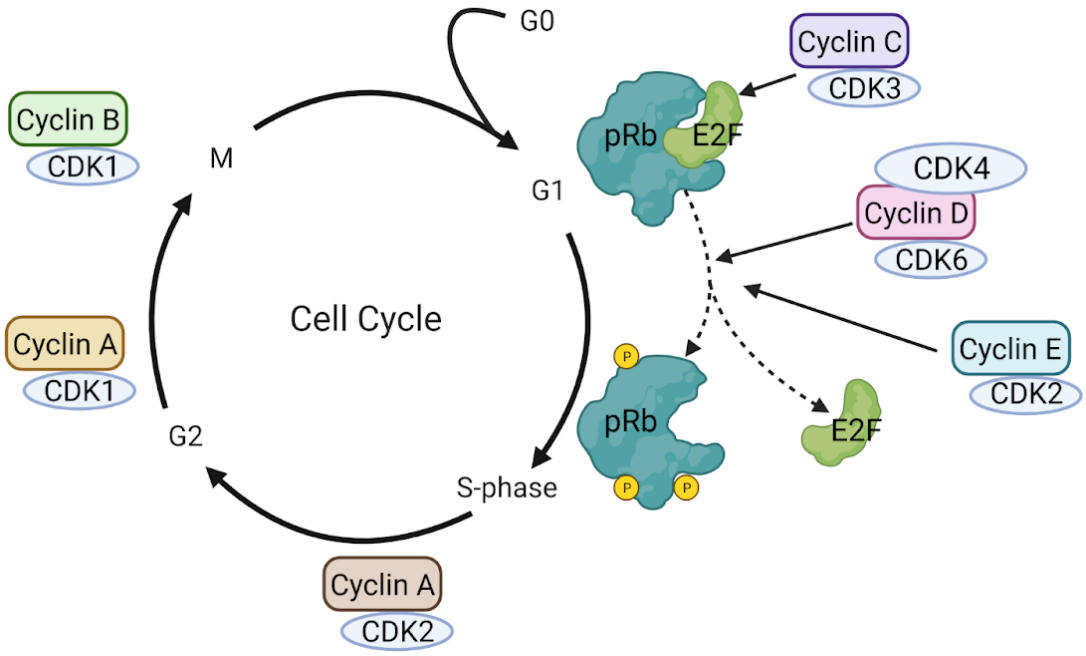

Figure 2: A visual representation of the cell cycle and the cyclin: CDK complexes. In G1 cyclin D: CDK4/6 directly interacts with pRb, activating transcription. This image also shows quiescence as a state that exists outside of the proliferative state. This image is based on an image from (Giacinti & Giordano, 2006).[14]

1.1 Cell Cycle

Cell division is the foundation of life and evolution. If a cell needs to enter the cell cycle, a signal is sent to the cell telling it to start growing. A cell starts the cell cycle in G1 when outside stimuli trigger cell division processes to start. In G1, the cell grows and replicates all non-nuclear parts of the cell. After the cell is of the right proportions, it turns on cell cycle genes in G1 to prepare for DNA synthesis. Right before the S phase, a cell passes through the R point to ensure the cell is ready for DNA replication. The restriction point (R point) is a limit where external signals are no longer required to trigger cell replication, and it is committed to the cell cycle.[15] In the S phase, the DNA is replicated. Once the DNA has been copied, a cell will enter the G2 phase before mitosis. In G2, there is another growth phase, and the organelles needed for mitosis are produced. The cell then proceeds into the M phase, and the cell finishes the process of dividing the nuclear components into opposite halves of the cell. Finally, cytokinesis occurs, and the membrane splits, resulting in two new daughter cells. While the widely accepted cell cycle model puts the R point in mid-G1, some experiments have shown that there could be a possible range for the location of the R point. The change in the R point location of the cell cycle could be due to variations in the cell type being used.[16] Despite its place in the cell cycle, the R point is where the cell becomes committed to the next round of cell division.

Throughout the cell division process, cyclins and Cyclin-Dependent Kinase (CDK) complexes control cell cycle checkpoints. They determine if the cell can move on to the next phase of cell division.[17] A different cyclin controls each phase of the cell cycle: Cyclin D regulates G1 before the R point by working with CDK 4/6, cyclin E

modulates G1 after the R point and the transition to G2 with CDK2, cyclin A controls S phase, as well as the G2 phase and M phase transition with CDK1/2, and cyclin B guides mitosis with CDK 1 (Figure 2). Our focus will revolve around the G1 checkpoint.

Two critical regulators of the cell cycle before the R point are pRb and p130 which assembles the DREAM complex. The cyclin D: CDK4/6 complex controls pRb and p130 phosphorylation, dictating if they can repress cell cycle gene transcription. Proliferation pathways are highly conserved for their importance to life and evolution. If any part of the regulatory system for cell replication fails, cells enter a state of unchecked proliferation, leading to cancer.[11]

1.2 Quiescence

All living organisms, from prokaryotes to humans, respond to changes in their environments that trigger cells to stop dividing. This lack of cellular division is called quiescence.[11] Importantly, quiescence, or G0, is a reversible state of the cell cycle, as compared to apoptosis or senescence, which are irreversible terminations of the cell cycle. Quiescence is also not a passive cell cycle phase but rather a maintained and highly regulated state.[18] Upon the discovery of the cell cycle in 1951 by Howard and Pelc, the cell cycle became widely studied. At this time Howard and Pelc also described cells that were not actively dividing. However, the G0 state was not officially characterized until 1974 when the R point was discovered.[18] Due to the early increase in cell cycle studies, the regulatory pathways of proliferation are understood far better than those of quiescence.[19]

In bacteria, dormancy is triggered by a lack of nutrients in the environment; However, in more complex organisms, such as mammals, cells do not have to be

nutrient-starved to quiesce. Instead, the cellular microenvironment can dictate if cells should replicate or not. Differentiated cells are typically quiesced and use catabolic metabolisms to obtain energy to perform cellular functions. If an organ or tissue becomes injured, mitogens signal the cells to reenter proliferation.[20] For example, skin cells are constantly replicating as dead cells brush off, while liver cells, which catalyze lipids and proteins, don't divide unless the liver becomes damaged.

Different types of quiescence exist depending on cell type, organism, or cell location.[11] Here we will focus on the quiescence of cancer cells. There are many hallmarks of cancer, and at the top of that list is unchecked proliferation. Despite uncontrolled growth being the most common sign of cancer, some cancers retain their ability to quiesce. The cause of quiescent cancer cells is unknown. While these quiescing cancer cells seem to be less of a threat because they have preserved some normal functions, this poses significant challenges when treating patients, since current treatments focus on killing cells in the cell cycle. Singular quiescing cancer cells that escape treatment can break off the primary tumor and get carried far away from the main tumor. Quiescent cancer cells can lay dormant for many years after completing cancer therapies. When these displaced quiescent cancer cells reenter proliferation, they cause metastasis and recurrent cancer.[21] Understanding the molecular triggers and pathways of quiescence in cancer cells will allow for more effective treatments against these quiescent cancer cells in the future. That process starts by studying the two direct regulators of quiescence, pRb and p130.

1.3 The DREAM Complex

The **d**imerization partner**, R**B-like**, E**2F, **a**nd **m**ulti-vulval class B **(**DREAM**)** complex is an intricate assembly of 8 proteins that regulate the expression of cell cycle genes (Figure 1). Evidence suggests that the DREAM complex plays a more prominent role in G0 regulation than G1 regulation, where pRb controls most of the regulation in G1.[5,22,23] This implies that DREAM is more involved in sustaining quiescence, while pRb regulates the exit from quiescence with unknown amounts of functional overlap.[24]

The DREAM complex consists of the p130 pocket protein that links E2F repressors and their DP binding partners to the MuvB core. The pocket protein p107 also forms the DREAM complex when p130 is nonfunctional, but p130 is the primary DREAM pocket protein.[6] The MuvB core consists of five proteins: LIN9, LIN37, LIN52, LIN54, and RbAp48 (Figure 1). LIN54 binds the MuvB core to the DNA, while LIN52 interacts with the pocket proteins (p130 or p107) that turn the MuvB core into the DREAM complex.[5] The DREAM complex interacts with repressive E2Fs, such as E2F4 and E2F5. However, E2F5 has a much lower expression than E2F4 in the cell.[7] E2Fs move throughout the cell depending on each cell cycle stage, but during G0 and G1, they are primarily accumulated in the nucleus by p130 and p107.[25] The assembled DREAM complex binds to the promoter region of DNA, acting as a transcriptional repressor to sustain quiescence. When a cell is ready to leave dormancy, the pocket protein becomes phosphorylated, and it dissociates from the MuvB core, which releases the E2F repressor. At this point, B-Myb can bind to the MuvB core (Figure 1). When B-Myb binds to the MuvB core, it creates the MMB complex, which activates transcription at the promoter of cell cycle genes needed for the G2/M phases.[26]

The cyclin D: CDK4/6 complex comes in and phosphorylates p130 when the cell is ready to leave quiescence. The phosphorylation of p130 disassociates it from the E2F4 repressor and the MuvB core. It is understood that pRb is also regulated in the same manner. The cyclin D: CDK4/6 complex phosphorylates pRb to disassociate it from the E2F activators at the promoter of the cell cycle genes. While p130 and pRb have remarkable similarities in structure and function, pRb is the dominant controller of the cell cycle in human cells. However, we cannot disregard the importance of DREAM's role in cell cycle regulation. The mutations in the DREAM complex that occurs when a cell becomes cancerous are unknown, and the DREAM complex may be the quiescent mechanism that is allowing cancer cells to quiesce.

1.4 The Retinoblastoma Protein

Isolated DNA from children's retinoblastoma cancers led to the discovery of the retinoblastoma protein in 1986. Gene sequencing analysis concluded that 95% of retinoblastoma tumors lose the retinoblastoma tumor suppressor protein (pRb). Since then, p130 and p107 have been discovered, creating the pocket protein family. p130, p107, and pRb have a highly conserved domain consisting of a two-part pocket structure.[27,28] They are highly conserved tumor suppressors that restrain cells from constantly proliferating to prevent DNA damage.[29] pRb binds to many different cell regulators and proteins, making its variety of specific functions in the cell largely unknown.[30] For our purposes, we will focus on pRb's interactions with the E2F transcription factor family, as they are integral to regulating cell cycle genes needed for the S phase. Both p130 and pRb bind to the E2F transcription factor family and their DP1 and DP2 binding partners for E2F1-E2F6.[2-3] The retinoblastoma protein suppresses E2F

transcription activators to control gene transcription. In higher-level organisms, such as humans, there are nine known E2F transcription factors; three are activators, and six are repressors. When pRb is unphosphorylated, it suppresses the E2F activators (E2F1, E2F2, and E2F3), preventing them from promoting transcription (Figure 2). E2F1 controls genes in G1 that are needed for the cell to pass the restriction point R to enter the S phase.[31,32] pRb can also bind to the repressor E2F4, but it cannot create the DREAM complex like p130 and p107.[33]

The retinoblastoma protein's interaction with E2F activators is controlled by phosphorylation. The field's phosphorylation model of pRb and p130 consisted of the proteins being gradually phosphorylated in early G1 until they reached a critical phosphorylation level where they dissociated from their E2F binding targets at the R point. In cells that are not dividing, pRb remains unphosphorylated, preventing transcriptional activation by E2F1.[34] Narasimha et al. experimented on 11 cell types to test if the phosphorylation model of pRb was correct. The cells were first synchronized into the G0/G1 phase. After being released from synchronization, they discovered that pRb is monophosphorylated after being released from G0. This mono-phosphorylated state lasted for the entirety of early G1. There was no evidence of multiple phosphorylations on pRb until 10 hours after the cells were released from synchronization: during late G1.[9] Furthermore, Narasimha et al. confirmed that the hyperphosphorylated state of pRb is sustained through the M phase and is then dephosphorylated completely by serine/threonine protein phosphatase-1 (PP1) after cytokinesis.[9]

1.5 Cyclins and CDKs and their Inhibition

Serum starvation and CDK inhibition are two methods used to test if a cell line can enter quiescence. Serum starvation occurs when nutrients are removed from the growth medium, and the cells stop dividing and enter G0. CDK inhibitors arrest cells by interfering with CDKs' ability to phosphorylate pRb and p130, which activates the proteins, synchronizing cells into G0. CDK inhibition can also lock cells into different phases of the cell cycle. This lock-in method can be useful for studying regulators at various checkpoints. As mentioned previously, several cyclin: CDK complexes work to modulate a variety of cellular replication processes. Cyclins bind to Cyclin-Dependent Kinases to activate the CDKs. Depending on which phase of proliferation a cell is in, cyclins are synthesized and degraded quickly.[36] There are 3 cell cycle checkpoints: the R point in G1, the G2 phase, and Anaphase in the M phase. These checkpoints ensure that the cell is large enough, has correctly synthesized DNA, and has proper chromosome formation. During the G0/G1 phases, cyclin D works in tandem with CDK4/6 to regulate proliferation via phosphorylation of p130 and pRb. In the later G1 and S stages, cyclin E works with CDK 2 to phosphorylate pRb to allow replication (Figure 2).[14]

pRb and p130 control the gene transcription of cyclin A and cyclin E, which move a cell from the late G1 stage to the S phase. Since cyclins modulate different phases of the cell cycle, they are quickly synthesized and degraded. In cells entering proliferation, the cyclin D: CDK4/6 complex phosphorylates pRb and p130, releasing them from the E2F family transcription factors, allowing transcription of cell cycle genes some of which encode cyclins A/E, progressing the cell cycle. [14]

1.6 Ovarian Cancer

According to the cancer statistics center, 21,410 women are predicted to be diagnosed with ovarian cancer in 2022, with the chances of a woman developing ovarian cancer in her lifetime being 1 in 78.[36] Epithelial ovarian cancer is cancer that arises in the outer layers of tissue that comprise the ovaries, and accounts for about 90% of all ovarian cancers.[37] There are two main subgroups of ovarian cancers: serous cell and non-serous carcinomas. The non-serous carcinomas consist of endometrioid, mucinous, clear cell carcinoma (CCC), and carcinosarcoma.[38] Non-serous ovarian cancer arises from endometriosis, which occurs from retrograde menstruation. Usually, menstrual blood flows from the uterus and out of the body. However, retrograde menstruation occurs when menstrual blood containing endometrial cells flows into the pelvic cavity.[39] There are two subcategories of serous ovarian cancer: high and low grade; high grade serous ovarian cancer arises from the fallopian tube fimbria and implants in the ovaries. High-grade serous cancers have a higher rate of mitosis, meaning they are much more aggressive than slower replicating low-grade serous ovarian cancers.[39] While high-grade serous carcinomas are more aggressive cancer types, late-stage non-serous cancers have a prognosis similar and sometimes worse than high-grade serous tumors. Despite their slower proliferation rate, if non-serous cancer grows unchecked, it can have dire consequences.[40]

Two standard ovarian cancer cell lines used in research are OVCAR3 and SKOV3. OVCAR3 is a high-grade serous ovarian cancer, and SKOV3 is a non-serous cystadenocarcinoma. Even though both of these cell types are epithelial ovarian cancers, they behave entirely differently. SKOV3 is a cell line that quiesces with serum starvation,

contact, and CDK inhibition, while OVCAR continues to replicate in those conditions.[12] OVCAR3 is considered a more aggressive cancer type than SKOV3 due to its rapid proliferation rates and ability to advance quickly *in vivo*. Since rapid proliferation is a hallmark of cancer, the mitotic process is often the primary target for chemotherapies; OVCAR3 is more likely to be killed by cancer treatments because it does not arrest and constantly proliferates. Chemotherapy typically targets cells in the cell cycle by inhibiting microtubules that catalyze division.[41-43] Due to SKOV3 cells' ability to quiesce, they can evade cancer therapies making them more likely to recur or to become metastatic.

It is widely accepted that cancer stem cells are primarily responsible for cancer drug resistance due to their ability to differentiate and self-renew. Ovarian cancer has given rise to cancer stem cells, creating a higher chance of recurrent cancer. These cancer cells can effectively evade cancer treatments through various stem cell pathways, such as quiescence, DNA damage repair, and anti-apoptotic pathways.[44] If cancer stem cells dissociate from the primary tumor, whether before or after cancer treatments, they can survive moving through the body until settling in a new location and restarting proliferation.[45,46] By determining the quiescence mechanisms and the individual roles of the DREAM complex and pRb, it could be possible to lock cells into a proliferating state where chemotherapy and cancer drugs can better target cancer cells.

1.7 CDK Inhibition of Ovarian Cancer

CDKs work to promote cell growth by phosphorylating proteins like pRb and p130, that would otherwise inhibit proliferation. CDK inhibitors were first used to treat estrogen receptor-positive, HER-2 negative breast cancer. Treatment with a CDK inhibitor caused sensitization of breast cancer cells to tamoxifen, a common breast cancer

chemotherapeutic.[47] Since then, CDK inhibitors have also been used to treat ovarian cancers.[48] Palbociclib, abemaciclib, and ribociclib are CDK inhibitors that interfere with a cell's ability to replicate. These CDK inhibitors block CDKs from phosphorylating pRb and p130. Unphosphorylated pRb and p130 proteins are active and prevent the cell from entering the cell cycle. Treating cells with CDK inhibitors allows us to lock them into G0, so we can study pRb and p130 during the transition from quiescence to proliferation.

1.8 Experimental Justification

We are interested in exploring why some cancer cells can quiesce. Because most cancers have mutated or missing retinoblastoma protein, the DREAM complex may be responsible for quiescent cancer cells.[28,49] As shown previously, there is a gap in knowledge surrounding the mechanism of cancer cells that can quiesce. Because the DREAM complex and Retinoblastoma protein work to suppress the cell cycle, it is possible they still function in cancerous cells. While the DREAM complex plays a significantly more minor role in cell cycle regulation than pRb, it overlaps greatly in function. Both proteins regulate the entry of the cell into the S phase by repressing cell cycle gene transcription, thus entering cells into and maintaining a cellular quiescence.[5,22,23,24,31,32] Even though pRb has been extensively studied since its discovery, there is still a gap in knowledge about its behavior in cell cycle regulation in cancerous cells. For this project, we were working with two ovarian cancer cell lines: OVCAR3, a high-grade serous carcinoma, and SKOV3, a non-serous cystadenocarcinoma. SKOV3 cells are known to serum starve and enter a quiescent state, unlike OVCAR3, which will continue to replicate even in the absence of serum.[50] To identify what complex is causing the shift from proliferation to quiescence in cancer cells, the two ovarian cancers will be

compared to human foreskin fibroblasts (HFFs), a non-cancerous cell line that we used as a control. To observe the cells at each phase of the cell cycle, we used a drug cocktail of palbociclib, abemaciclib, and ribociclib (PAR) to arrest the cells in G0 and we used nocodazole to arrest cells in G2.[14,18] We used flow cytometry to observe if each cell line responded to the drug treatments, and to make sure we were harvesting the cells at the correct time to isolate the desired cell cycle phase. We would expect the HFF and SKOV3 cells to quiesce in response to the PAR treatment, and OVCAR3 cells do not respond to the PAR treatment since they do not quiesce. Flow cytometry sorts cells into two categories: pre-DNA replication and post-DNA replication. Then Western blots were used to visualize the presence of pRb and p130. If the proteins are both present in the cell lines, Real-time-quantitative PCR (RT-qPCR) was performed to analyze cell cycle gene expression as a way to identify potential malfunctions of pRb and p130.

2 Methods

2.1 CDK Inhibition of Cells

We used a cocktail of CDK inhibitors: palbociclib, abemaciclib, and ribociclib (PAR) as well as nocodazole to treat the cell lines. The PAR drug cocktail has 33 nM palbociclib, 33 nM abemaciclib, and 167 nM ribociclib.[51] Abemaciclib and ribociclib both inhibit the cyclin D: CDK 4/6 complex, while palbociclib inhibits both the cyclin D: CDK 4/6 complex and the cyclin E: CDK 2 complex. Adding PAR to the cell culture for 24 hours locks the cells into a G0/G1 phase, i.e., the cell is quiescent. The time points of interest in the cell cycle are G0/G1, late G1, S phase, and G2. We isolated the proliferating sample by growing cells in normal serum media for 24 hours before harvesting them. The G0/G1 sample was collected by adding the PAR drug cocktail to the media for 24 hours before harvesting the cells. To isolate the late G1 and S phases, the cells were treated with PAR for 24 hours. After 24 hours, PAR was removed, and replaced with normal serum media for 6 hours and 11 hours to harvest late G1 and the S phase, respectively. To isolate the G2 phase, the cells were treated with PAR treatment for 24 hours. After 24 hours the PAR treatment was removed, and nocodazole was added. After an additional 24 hours, the G2 sample was harvested. Nocodazole is a drug that inhibits mitotic spindle formation, which arrests the cell before it can divide, in the G2 phase.

2.2 Flow Cytometry

350,000 cells were added to each well of a 6 well plate and allowed to settle for 24 hours before the PAR and nocodazole treatments were added. Each plate was harvested by adding 250 μL of trypsin to each well and incubating them at 37℃ for 5 minutes.

After 5 minutes, we added 750 µL of growth medium and transferred it to individual 1.5-mL tubes. We spun the samples down at 4,000 rotations per minute (rpm) for 2 minutes. We removed the liquid and added 1 mL of PBS. We spun down the samples again at 4000 rpm for 2 minutes. Then we removed most of the liquid but left about 50 µL. We pipetted the pellet up and down with a p200. Then we added 500 µL of ice-cold 70% ethanol and stored it in the -20℃ freezer. The night before flow, we thawed and spun the samples for 2 minutes at 4,000rpm at 4℃. We discarded the supernatant and resuspended the cell pellet in 500 µL of PBS containing 0.25% Triton X-100, and incubated it for 15 minutes. We spun the cells down again for 2 minutes at 4,000 rpm and 4°C. We discarded the supernatant and resuspended the cell pellet in 500 µL of PBS containing 10µg/mL RNase A and 20 µg/mL propidium iodide stock solution. We then transferred the samples to FACS tubes and incubated them at room temperature in the dark overnight. After overnight incubation, the samples were run on the NXT Attune Flow Cytometer in the CIF at Michigan Technological University.

2.3 mRNA Isolation

We started by adding approximately 1.5 million cells to a 10 cm^2 plate. When the cells were ready to harvest we added 1 mL of Trizol. The plates were scrapped and each sample was put into two 1.5-mL tubes with 500 uL of trizoled cells in each. They were stored at -70℃, and thawed completely. Then we added 100 µL of chloroform to each sample. The samples were vortexed and we transferred all the liquid to 2 mL phase-lock tubes. We spun the tubes down at 4℃, 12,000 Relative Centrifugal Force (RCF) for 15 minutes. We then transferred the aqueous layer to a new 1.5-mL tube and added 250 µL of isopropanol and vortexed the samples. We let them incubate for 5 minutes at room

temperature. We spun the samples down at 4℃, 12,000 RCF for 8 minutes. Then we discarded all of the liquid, careful to not disturb the pellet at the bottom. 750 µL of 75% ethanol was added, and we spun the samples down at 4℃, 12,000 RCF for 5 minutes. We discarded the supernatant carefully so that the pellet was not disturbed. Then we spun down the samples again for 1 minute, removed the remaining liquid, and let the tubes air-dry for 3 minutes. Finally, we added 20 µL of nuclease-free water and stored the samples in the -70℃ freezer for at least 1 hour to overnight.

2.4 Nanodrop Quantification

We removed the samples from the freezer and heated them at 60℃ for 20 minutes. Then we placed them on ice. We measured 1.5 µL of RNA on the Nanodrop and recorded the ng/ µL. The ideal content was >150 ng/µL of RNA. If samples were above 2000 µg/µL, we diluted them to approximately 1000 µg/µL.

2.5 RT-qPCR

We started by diluting the RNA to 1 µg by adding X µL of RNA to a new PCR tube (X=1000/RNA content). We then diluted the RNA again to 11 µL with nuclease-free water. Next, we created the RT-PCR master mix, as per manufacturer instructions for the applied biosystems kit by Thermo Fisher Science. We then added 9 µL of the RT-PCR master mix to each sample, bringing the total volume to 20 µL. We spun the tubes down briefly, and ran the samples in the Fischer Sciences Thermocycler at 25℃ for 10 min, 37℃for 120 minutes, 85℃ for 5 min, and then held at 16℃. When the samples were done running, they were stored overnight in the -20℃ freezer.

On the next day, we thawed the samples and moved each sample into a new 1.5-mL microcentrifuge tube. We diluted the samples with 180 µL of ddH_20 to bring the volume up to 200 µL. In a 96-well PCR plate, we added 2 µL of cDNA and 18 µL of PCR master mix, prepared according to manufacturer instructions for the applied biosystems kit by Thermo Fisher Science. Each primer set we used had a master mix. We sealed the 96-well PCR plate with a sticker, ensuring all of the sides are thoroughly sealed. We then spun down the PCR plate for 1 min to ensure all reagents are at the bottom of the tube. We saved the experiment and ran the experiment: 50℃ for two minutes, 95℃ for 10 minutes 15 seconds, 60℃ for one minute repeated for 40 cycles on the QuantStudio machine by Thermo Fisher Science.

2.6 Western Blots

We started with 2 plates of cells seeded with about 1.5 million cells and harvested the protein from the sample by washing each cell plate with 5 mL of cold 1x PBS. Everything was kept as cold as possible by working on ice the entire time. We then added another 1 mL of PBS and scrapped the cells into 1.5-mL microcentrifuge tubes. We spun the cells down at 4°C, 2,000 rpm for 2 minutes. We discarded the supernatant, and resuspended the cells in 400 µL per plate of buffer A: 10 mM Tris-HCl, pH 8.0; 1 mM EDTA; 0.5 mM EGTA; 1% Triton X-100; 0.1% Sodium Deoxycholate; 0.1% SDS; 140 mM NaCl; and 1 mM PMSF. We combined each condition into a single tube. We incubated the tubes for 10 minutes on ice. Then we spun the tubes at 4°C, 5,000 rpm for 2 minutes to pellet the nuclei. After we removed supernatant, and we gently resuspended the pellet in 100 µL of buffer C:50 mM Hepes-KOH pH 7.8; 420 mM KCl; 0.1 mM EDTA; 5 mM $MgCl_2$; 1 mM DTT; and 0.5 mM PMSF. We set the samples on a rotator

shaker for 30 minutes in the 4°C fridge. We spun the cells down at 4°C, 13,000 rpm for 15 minutes. Then we transferred the supernatant to a new microcentrifuge tube and kept them on ice.

While samples sat on ice, we prepared the qubit working solution. We made 200 µL of Qubit protein buffer per sample and an additional 600 µL for the standards. For the standards, we added 190 µL of working solutions and 10 µL of standards. For the samples, we mixed 198 µL of working solution and 2 µL of protein isolate. After the protein concentration was determined, we diluted the samples the same concentration of the least concentrated protein using buffer B: 10 mM Hepes-KOH pH 7.8; 10 mM KCl; 0.1 mM EDTA; 5 mM $MgCl_2$; 20%v/v glycerol; 1 mM DTT; and 0.5 mM PMSF. The samples were stored in the -70°C freezer until their next use.

We prepared the western protein gel mold and filled it with ethanol to ensure the apparatus did not leak. In a 50 mL beaker, we prepared the 12% 10 mL resolving gel: 4.0 mL of 30% acrylamide mix, 2.5 mL 1.5 M TRIS pH 8.8, 3.3 mL of ddH_2O, 0.1 mL 10% SDS solution, 0.1 mL 10% ammonium persulfate (APS), and 8.0 µL TEMED. We swirled each reagent to mix after adding it to the beaker. We then removed the ethanol from the gel mold by flipping the mold upside down and letting the ethanol drain out completely. We used a p1000 to add 4 mL of resolving gel to the mold, and then we added 1 mL of tert-butyl alcohol on top to ensure an even gel surface. We kept leftover gel liquid in the beaker to determine when the gel had solidified. In the meantime, we prepared the 4 mL stacking gel in a new 50 mL beaker: 0.67 mL of 30% acrylamide mix, 2.7 mL ddH_2O, 0.5 mL of 1 M TRIS pH 6.8, 40 µL of 10% SDS, 40 µL 10% APS, 8 µL

of TEMED. The TEMED was added last, and the more TEMED added, the faster the gel solidifies. APS was made freshly every time to ensure proper gel solidification. Then we remove all of the tert-butyl alcohol by flipping the apparatus upside down after the gel has completely solidified. We added 1.5 mL of stacking gel solution and inserted well combs, and let them solidify.

In the fume hood, we mixed 200 µL of BME into 1 mL of SDS loading buffer. In newly labeled tubes, we mixed 50 µL of protein samples with 50 µL of SDS/ BME loading buffer and heated the samples to 98℃ for 4 minutes. We then placed the remaining protein samples into the -70℃ freezer for storage. Once the gel completely solidified, we removed the gel casing from the apparatus and placed it in the gel running chamber, careful to face the front of the gel towards the middle of the chamber. We filled the chamber with a 1x SDS loading buffer and filled the outside of the chamber to either the 2 or 4 gel mark- depending on how many gels were being run. We removed the well mold by gently pulling it straight up, and then cleaned the wells out by using the p1000 to pipette loading buffer into each well several times. We loaded 2.5 µL of protein ladder into the first well, and then we loaded the samples into the rest of the wells. Any empty wells were filled with SDS loading dye. We ran the gel at 100 V for the first 20 min and then at 200 V until the dye reached the bottom of the gel. After running the gel, we removed it from the case and transferred it into a container with transfer buffer, and stored them overnight at 4℃ if needed.

We filled a small bucket with transfer buffer and placed the black side of the transfer clamp in the buffer. We added the black sponge, and then a piece of filter paper on top of the sponge. We removed the stacking gel from the running gel and placed the

protein gel on top of the filter paper. We activated the PVDF membrane by soaking it in methanol for 1-2 seconds before placing it on top of the gel. We thoroughly removed all of the bubbles between the gel and the membrane. We covered the membrane with another piece of filter paper and removed all of the air bubbles. We placed another sponge down before closing the transfer clips. We placed the transfer apparatus into the chamber so that the black side was facing the black wall and the clear side was facing the red wall. We filled the running chamber with transfer buffer, and we ran the transfer at 100 V for one hour. We set an hour timer on the voltmeter as the transfer cannot go for longer than one hour. After the transfer, we removed the membrane from the transfer apparatus and flipped the membrane so the protein-containing side faced upward. The protein content was then checked using the total Q stain. We made a 5% milk stock solution with 5 g powdered milk in 100 mL of PBST. We placed the membrane into the black box and added 5 mL of 5% milk to block the membrane. We placed the membranes on the rocker at 50 rpm at room temperature for an hour. Then we removed the milk and added 4 mL of 5% milk containing antibodies. We placed the box on the rotator in the fridge overnight. The next morning, we removed the antibody milk from the membrane and washed the membrane 3 times with PBST for a minimum of 5 minutes each wash. Then we added 4 mL of 5% milk and then added 1 µL of the secondary mouse or rabbit antibody- depending on what type of primary antibody is used. We let the secondary antibody shake at room temperature for 2 hours at 50 rpm. Then we removed the secondary antibody and washed it with PBST three times for 15 minutes each at room temperature on a rocker at 50 rpm. In a glass tube, we mixed 500 µL of Thermo scientific Stable peroxide solution with 500 µL of Thermo scientific Luminol/enhancer solution per

membrane, 1 mL total for each membrane. We swirled by hand for a few seconds to mix, and then we removed the membrane with forceps and blotted excess liquid by touching the edge of the membrane to a paper towel. We placed the membrane onto a piece of plastic wrap and sealed the membrane. We then put the membrane on the black tray and placed the tray into the azure imaging machine. Use the CHEMI BLOT setting to image the membrane.

For phosphorylated western blots, we replaced PBS with TBS. The TBS was then used to make a 5% solution with bovine serum albumin as a replacement for the 5% milk solution. The TBST was used for the wash steps.

2.7 Chromatin Immunoprecipitation

Starting with treated cell plates that were seeded with about 1.5 million cells, we removed the medium and added 4 mL of 1.5% formaldehyde in PBS to each plate. We shook the plates at 40 rpm for 15 minutes. We then added 400 µL of 1.25 M glycine and shook them for 5 more minutes. The plates were then scraped into tubes, washed with NCP buffer #1:10 mM EDTA, 0.5 mM EGTA, Hepes 10 mM pH 6.5, and Triton X-100 0.25%; then NCP buffer #2:1 mM EDTA, 0.5 mM EGTA, Hepes 10 mM pH 6.5, and 200 mM NaCl. After we removed the second buffer, we added the lysis buffer:10 mM EDTA, 50 mM Tris-HCL pH 8.1, 0.5% Empigen BB, and 1% SDS. We then sonicated the cells with the Branson tip sonicator for 25 seconds three times. The amplification was set to 15%. After sonication, we spun the samples down at max speed for 10 minutes, and then added 20 µL of Dynabeads protein A to preclear for an hour. We then placed the samples on a magnet rack, and the supernatant was put into a new labeled tube and split so there is 100 µL of supernatant per antibody sample plus 100 µL for sizing and input samples.

Chip buffer: 2 mM EDTA, 150 mM NaCl, 20 mM Tris-HCl pH 8.1, 1% Triton X-100, and protease inhibitors were added to the samples. Antibodies were also added to the samples and left to mix in the 4℃ fridge overnight.

The next day, we added 10 µL of Dynabeads protein A to the samples, and the samples were placed back on the rotator for an hour. The samples were then washed once with wash #1 (2 mM EDTA, 20 mM Tris-HCl pH 8.1, 0.1% SDS, 1% Triton X-100, and 150 mM NaCl), wash #2 (2 mM EDTA, 20 mM Tris-HCl pH 8.1, 0.1% SDS, 1% Triton X-100, and 150 mM NaCl), and wash #3 (10 mM Tris-HCl pH 8.1, 1 mM EDTA, 250 mM LiCl, 1% Deoxycholate, and 1% NP-40). Next, we put the supernatant into a new tube after the first wash. Then we washed the samples twice with TE buffer: 10 mM Tris-HCl pH 8.1, and 1mM EDTA. After all of the washes, we added the elution buffer (1% SDS and 0.1 M NaHCO3) to each sample. The samples were then heated at 55℃ for 15 minutes. We removed the supernatant, placed it into a new tube, and added 50 µL more elution to the beads. The samples sat at 55℃ for 15 more minutes, and then we transferred the supernatant to the new tubes for a total of 100 µL. We added 4 µL of 5 M NaCl. We placed the samples in the thermocycler overnight at 65℃.

The next day we added 100 µL of phenol-chloroform to each sample and we vortexed to mix for 10 seconds. The samples were then spun down and ~90 µL of the aqueous layer was removed. We then put the samples into a new final tube. To each tube, we added 10 µL of NaOAC, 1 µL 20/20 glycogen, and 250 µL of 100% ethanol. The samples were placed in the -20℃ freezer overnight. The next morning, we spun the samples at full speed for 30 minutes at 4℃. We washed the pellet twice with 500 µL of ice-cold 75% ethanol, spinning at 4℃ for 10 minutes between washes. Once the ethanol

was removed, we air-dried the samples for 4 minutes. The pellet was resuspended in 50 µL of nuclease-free water, and the sample was stored in the -20℃ freezer.

3 Results

3.1 HFF and SKOV3 cells respond to PAR CDK inhibition

We were interested in determining if the CDK inhibition cocktail of palbociclib, abemaciclib, and ribociclib (PAR) affect the cell cycle in HFF, SKOV3, and OVCAR3 cells. We used propidium iodide to observe the number of cells in a population that are in G0/G1 (2n) and the number of cells in a population that are in G2 (4n). The G0/G1 population appears in a peak on the left followed by the G2 peak appearing on the right. Cells that are in S phase appear between the two primary G0/G1 and G2 peaks. If the cells respond to the CDK inhibition, we can assume they can enter quiescence, and that pRb and p130 retain at least some of their function and can suppress cell cycle gene transcription. As we release the cells from the PAR treatment, we expect to see the cells reenter the cell cycle indicating that the cyclin D: CDK 4/6 complex can phosphorylate pRb and p130. As the cells continue into S phase, we expect to see the cells between the two primary peaks, signifying that pRb and p130 dissociated, and the cell was able to pass through the R point and continue into DNA replication.

We observed that the HFF cells did respond to the PAR drug cocktail by arresting in G0/G1 following 24 hours of PAR treatment. The PAR treatment shows a smaller cell population in the G2 phase with most of the cells being enriched in the first peak. This result suggests that the majority of the population was entering the quiescent state, and pRb and p130 are functioning. Six hours after the cells were released from PAR treatment, there was a shift in the population, and the second G2 peak became more enriched, indicating that the cyclin D: CDK 4/6 complex was phosphorylating p130 and pRb. Eleven hours post PAR treatment, the space between the primary peaks was

enriched, suggesting the cells were moving through the S phase of the cell cycle. To lock the cells into the G2 phase, nocodazole was added directly after the completion of the 24-hour PAR treatment. In the P+N image, the second peak was much more enriched; however, there was a considerable portion of the population in the G0/G1 state. This suggests that the HFF cell time course may need to be altered in the future to better isolate the phases of the cell cycle (Figure 3).

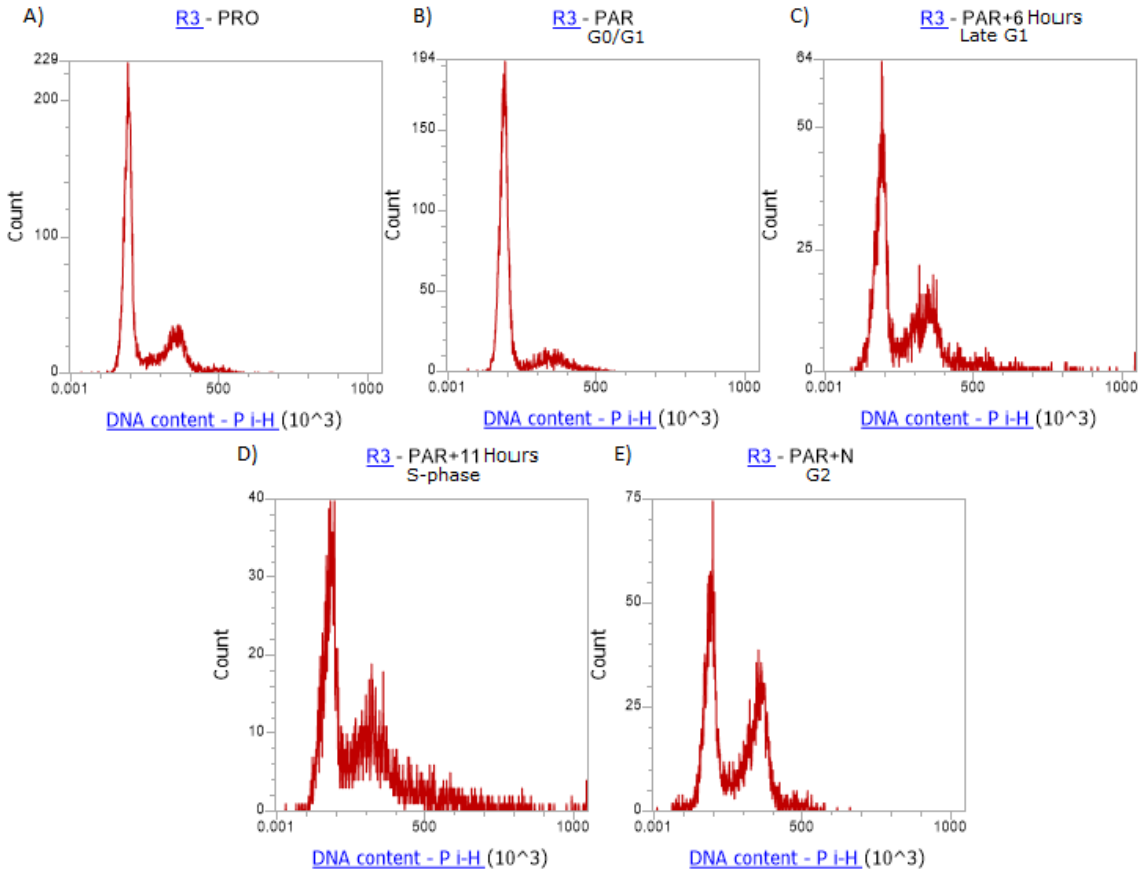

Figure 3: Flow cytometry cell cycle sorting of the HFF cells. A) The PRO sample shows unsynchronized cells moving through the cell cycle at random which is seen by the two primary G1 (left) and G2 (right) peaks. B) In the PAR graph, the cells are synchronized into the G0/G1 state by the CDK inhibitors. This is seen by the decrease in the size of the G2 peak. C) The PAR + 6 hours shows the cells in the late G1 state as they start to move through the cell cycle. This is indicated by the increase in the size of the G2 peak. D) The PAR + 11 hours image depicts the cells moving through the S phase. The S phase is indicated by the area between the two primary peaks. F) The last image shows the G2 phase as the cells were treated with PAR and Nocodazole, and is indicated by the increase in the size of the G2 peak. Each sample had three biological replicates.

In the SKOV3 cells, (Figure 4) we observed a shift in the cell population to G0/G1 after the 24-hour PAR treatment as compared to the treatment-free proliferating cell population. This result suggests that the cell population was entering the quiescent state. Since the cells appear to be in a quiescent state, that would mean either pRb or p130 or both are functional in some capacity. Six hours post PAR treatment, the cell population began to shift to the second G2 peak, suggesting the cells were leaving quiescence and reentering cell division. This result suggests that cyclin D: CDK4/6 was able to phosphorylate pRb and p130 in some capacity. Eleven hours post-treatment the population of cells was largely enriched between the two primary peaks. This observation supports the notion the cells were in the S phase. In the PAR-and nocodazole-treated SKOV3 cells, most of the cell population was present in the G2 peak, while very few cells were present in the G0/G1 peak, suggesting that the cells are nearing division. The SKOV3 cells had the most intense reaction to the CDK inhibition, which indicates the correct time course for collecting the different phases of the cell cycle.

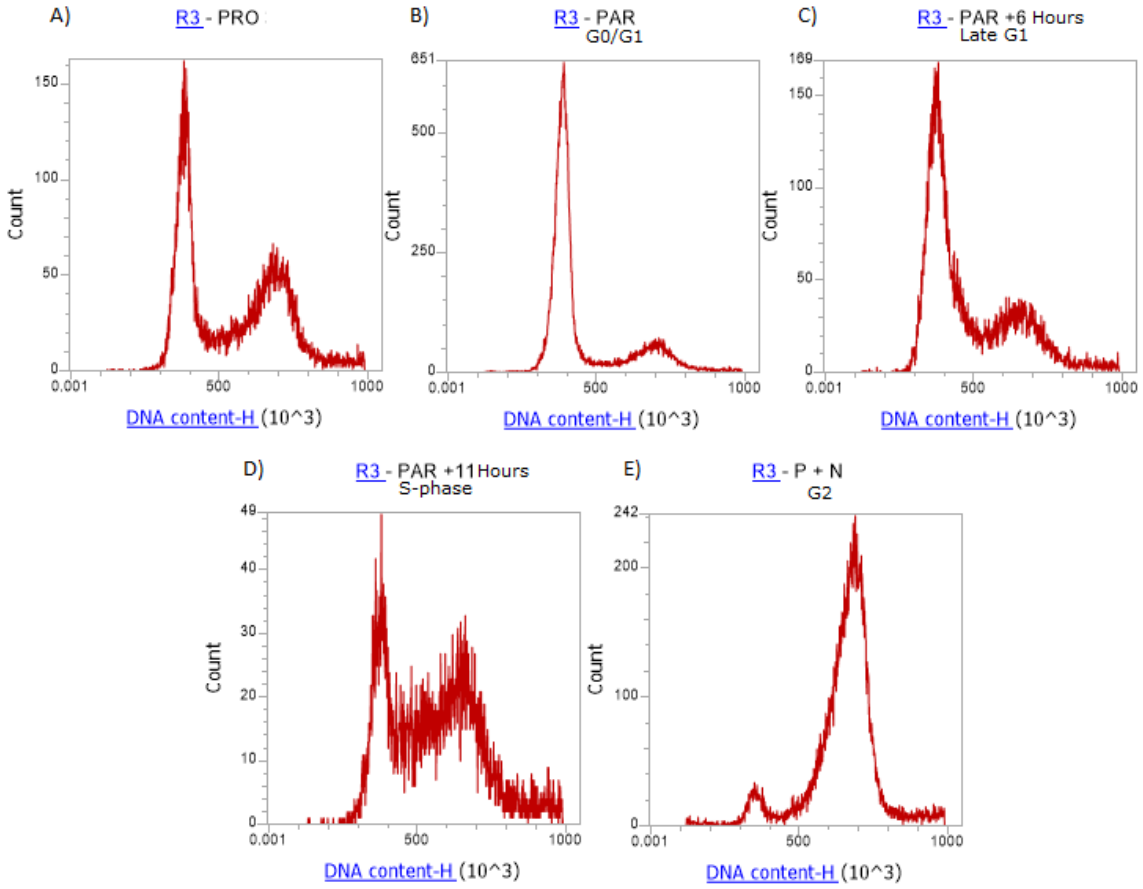

Figure 4: Flow cytometry cell cycle sorting of the SKOV3 cells. A) The PRO sample shows unsynchronized cells moving through the cell cycle at random which is seen by the two primary G1 (left) and G2 (right) peaks. B) In the PAR graph, the cells are synchronized into the G0/G1 state by the CDK inhibitors. This is seen by the decrease in the size of the G2 peak. C) The PAR + 6 hours shows the cells in the late G1 state as they start to move through the cell cycle. This is indicated by the increase in the size of the G2 peak. D) The PAR + 11 hours image depicts the cells moving through the S phase. The S phase is indicated by the area between the two primary peaks. F) The last image shows the G2 phase as the cells were treated with PAR and Nocodazole and is indicated by the increase in the size of the G2 peak. Each sample had three biological replicates.

The OVCAR3 cells, (Figure 5) did not respond to the PAR treatment. After the 24-hour PAR treatment, the population of the OVCAR3 cells remained unchanged, with most of the population in the G0/G1 peak and a smaller portion of the population in the G2 peak. Both the six and eleven-hour post-PAR treatments were also unchanged from the proliferating sample. However, after nocodazole treatment, the OVCAR3 cells did respond. Most of the cell population switched to the G2 peak, where the nocodazole interrupts the microtubules, resulting in the G2 arrest of cells. The CDK inhibitors did not affect the OVCAR3 cells, which was expected.[50] Therefore, we were unable to further observe the exit of quiescence in the OVCAR3 samples. This inability to respond to CDK inhibition of the cyclin D: CDK 4/6 complex suggests that the OVCAR3 cells either have missing or dysfunctional pRb and p130 proteins, which we investigated with Western blots.

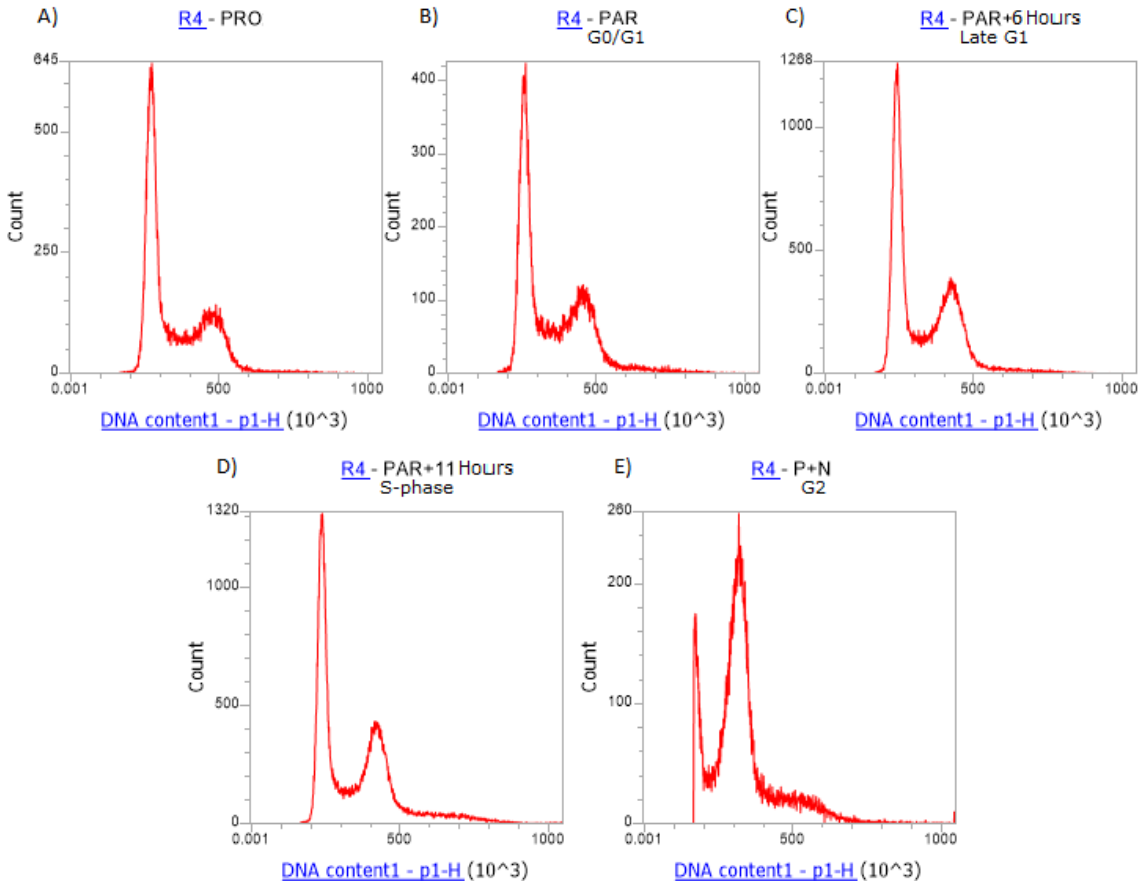

Figure 5: Flow cytometry cell cycle sorting of the OVCAR3 cells. A) The PRO sample shows unsynchronized cells moving through the cell cycle at random which is seen by the two primary G1 (left) and G2 (right) peaks. B) In the PAR graph, the cells do not respond to the PAR treatment, no change is seen in the size of the peaks from the PRO image. C) The PAR + 6 hours shows the cells do not respond to the PAR treatment, no change is seen in the size of the peaks from the PRO image. D) The PAR + 11 hours image depicts the cells that do not respond to the PAR treatment, no change is seen in the size of the peaks from the PRO image. F) The last image shows the G2 phase as the cells were treated with PAR and Nocodazole and is indicated by the increase in the size of the G2 peak. Each sample had three biological replicates. Each sample had three biological replicates.

3.2 p130 is under expressed in OVCAR3 cells

We were interested in evaluating if p130 and pRb were present at each phase of the cell cycle- G0/G1, late G1, S phase, and G2 as well as proliferating samples. If one of the proteins is absent in SKOV3, then we know which protein is responsible for the cells entering quiescence. The HFF and SKOV3 cells responded to the PAR treatment, but OVCAR3 did not, so only OVCAR proliferating samples were collected and compared to SKOV3 and HFF proliferating samples (Figure 6). After isolating the nuclear protein fraction, the proteins were separated on a gel and then transferred to a membrane. Anti-RB and anti-p130 antibodies were used to tag pRb and p130. If the proteins are present in a sample, a band will be present at 106 kDa for pRb and 130 kDa for p130.

To observe protein presence in each cell line, we started with a Western blot with only proliferating samples for the HFF, SKOV3, and OVCAR3 cells. In the pRb Western blot, we saw a band in each proliferating sample, indicating that pRb is present in all of the cell lines (Figure 6). In the p130 Western blot, we saw a protein band in both the HFF and the SKOV3 samples. The OVCAR3 sample, however, contained very little if any protein band, despite the OVCAR3 samples having the highest protein isolate concentration (Figure 6). These results indicate that pRb is non-functional in the OVCAR3 cells because p130 is not present and the OVCAR3 cells do not respond to the PAR treatment.

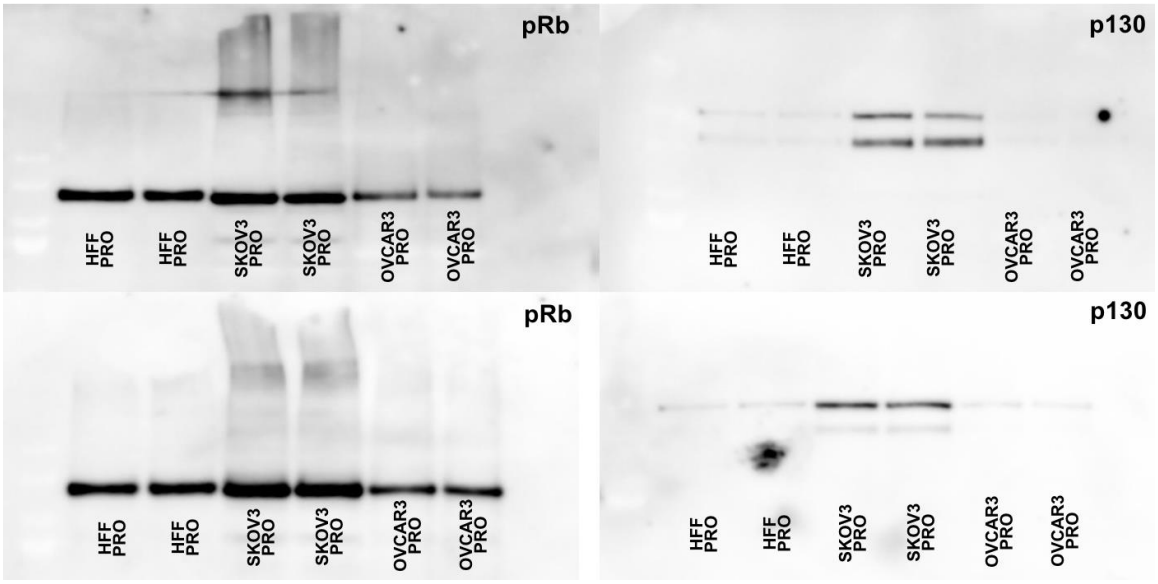

Figure 6: Western blots of pRb (left) and p130 (right) of HFF, SKOV3, and OVCAR3 proliferating samples. On the left, HFF, SKOV3, and OVCAR3 samples, respectively, were tagged with anti-pRb antibodies. On the right, HFF, SKOV3, and OVCAR3 samples were tagged with anti-p130 antibodies. There are two samples for each cell line with two technical replicates.

To further investigate if pRb and p130 are present in the HFF and SKOV3 cells, we harvested the cells at each time point for the cell cycle: G0/G1, late G1, S phase, and G2. In the HFF cells, we detected pRb and p130 present in all of the time points. The protein band in the late G1 SKOV3 sample shows a much lighter band in the PAR +6 sample. This could be due to the phosphorylation of the protein as it enters the cell cycle (Figure 7A). The p130 bands are fainter than the pRb bands, suggesting a higher quantity of pRb in the cells (Figure 7B). In the HFF cells, we observed pRb to be present at all time points of the cell cycle. In the HFF p130 Western blots, we saw p130 at every time point with a decrease in band intensity at PAR + 6 hours, which could indicate p130 inactivation due to cyclin D: CDK4/6 phosphorylation (Figures 7 C and D).

We further investigated the presence of phosphorylated pRb and p130 in the SKOV3 samples with phospho-Westerns. Using phosphorylation-specific antibodies to identify if the unphosphorylated pRb and p130 disappear. We expected to see the unphosphorylated pRb and p130 disappear in the PAR treated samples since the cells are synchronized into the G0/G1 state.[9] We expected to see the phosphorylated pRb and p130 reappear starting in late G1 at the PAR+ 6-hour time point. At the late G1 phase, the cyclin D: CDK 4/6 complex has started phosphorylating pRb and p130, and the cell starts to prepare for DNA synthesis. We observed phosphorylated pRb at every time point (Figures 7 E and F). This result indicates potential dysfunction of pRb in the SKOV3 cells. We expected to see no phosphorylated protein in the PAR treated cells that were synchronized into G0/G1. Because there is some inactivated pRb in the cell when it is supposed to be active, this could lead to cell cycle genes being expressed when the cell is in quiescence.

There was not enough protein for the HFF proteins to appear on the phosphor-Western blot, so they are not shown.

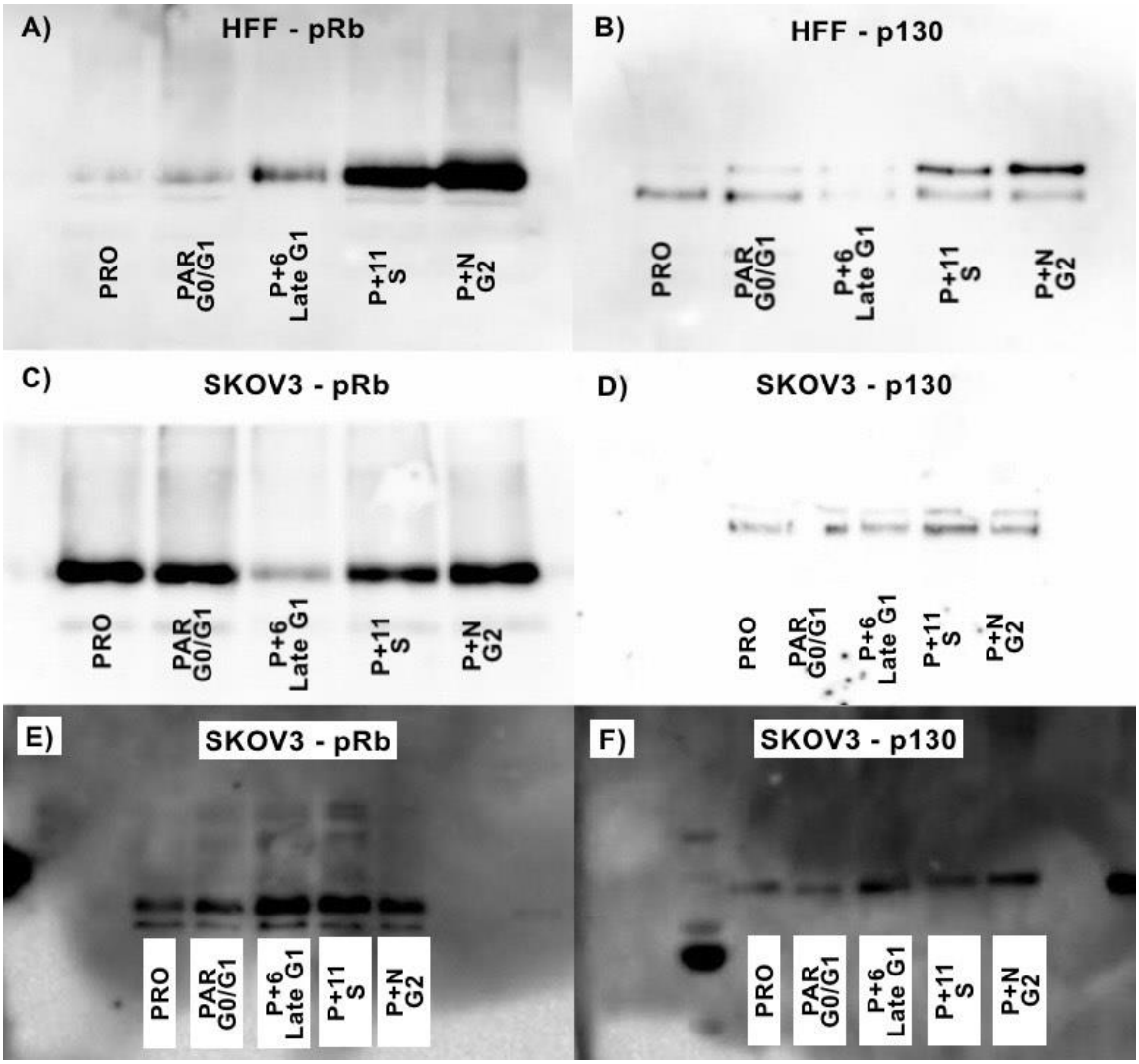

Figure 7: Western blots of pRb (left) and p130 (right) are shown in the HFF cells (A and B) and SKOV3 cells (C and D). In SKOV3 and HFF cells each of the 5 time points is shown: proliferating, G0/G1 (PAR treated), late G1 (PAR treated + 6 hours), S phase (PAR treated + 11 hours), and G2 (PAR treated + Nocodazole), from left to right. Phospho-western of the SKOV3 time course is shown with proliferating, G0/G1 (PAR treated), late G1 (PAR treated + 6 hours), S phase (PAR treated + 11 hours), and G2 (PAR treated + Nocodazole), from left to right (E and F).

3.3 Expression Analysis Using RT-qPCR

Because we were able to determine that pRb and p130 were present in both the SKOV3 and the HFF samples, we were interested in testing the mRNA expression of the cell cycle genes that pRb and p130 regulate. We used mRNA isolated from the HFF and SKOV3 at each time point and proliferating OVCAR3 cell samples. We converted the mRNA to cDNA with reverse transcription. We then ran a qPCR using the hβ-actin and hU6 housekeeping genes as a control. Housekeeping genes are genes that are required for the maintenance of basic cellular functions that are usually always expressed. We compared the mRNA expression of two cell cycle genes: hCCNB2 and hMCM5 to the mRNA expression of two housekeeping genes. We expect hCCNB2 to be present in the late cell cycle, and hMCM5 to be present in the S phase of the cell cycle. We compared each time point to the synchronized G0/G1 cells that were PAR treated. For our negative control, when we compared the two housekeeping genes, we saw no significant changes at any point in the cell cycle for the HFF cells, as expected. There were also no significant changes in the SKOV3 cells at any cell cycle phases (Figure 8).

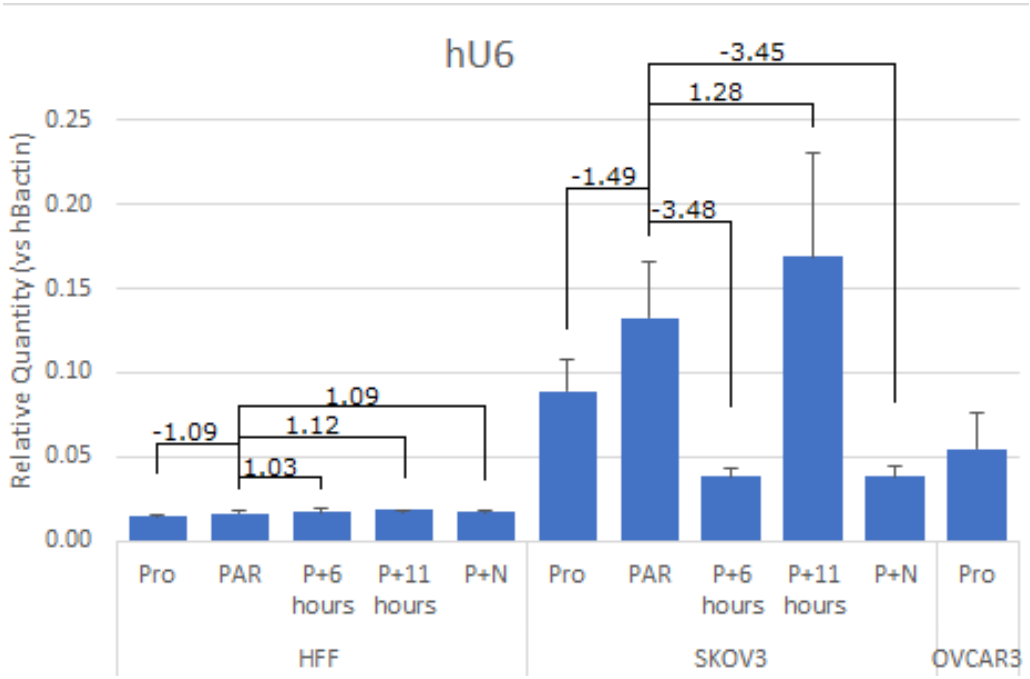

Figure 8: RT-qPCR gene expression analysis of the hβ-actin and hU6 negative control. Each treatment, proliferating, PAR (G0/G1), P+6 hours (late G1), P+11 hours (S phase), and P+N (G2), are shown from the left to right respectively for both HFF (left) and SKOV3 (right). Each cell cycle phase was compared to the cells arrested in the G0/G1, PAR condition for HFF and SKOV3 cells. * indicates <0.05 and ** indicates <0.01 p-value.

We next looked at the mRNA expression of hCCNB2 compared to hβ-actin. hCCNB2 is a gene present in the late cell cycle.[52] We saw a significant 2.0- and 2.7-fold increase from PAR treated HFF cells in both the proliferating sample and the PAR +11 hour samples, respectively. However, in the SKOV3 cells, there was a 3.7- and 2.6-fold significant increase in the PAR + 6 hours and PAR +11 hours SKOV3 cells, respectively (Figure 9). The lack of significant fold change between the proliferating sample and the PAR treated G0/G1 SKOV3 sample indicates dysfunction in either the pRb or p130 proteins' ability to repress the cell cycle genes during quiescence.

We then looked at hMCM5 in comparison to hβ-actin. hMCM5 is a cell cycle gene present in the late cell cycle.[53] We saw significant increases in expression in the proliferating, PAR + 11-hour S phase, and P+N G2 HFF samples. The significant increases from the PAR G0/G1 synchronized cells were 3.4-fold, 2.7-fold, and 8.2-fold, respectively. However, in the SKOV3 samples, there was only a significant increase in mRNA expression for the proliferating samples. The mRNA expression increase from the PAR G0/G1 samples was only a 2.2-fold increase (Figure 10). Because the fold change in the SKOV3 proliferating sample was less than the fold change in the HFF sample, that could indicate an inability of pRb or p130 to reduce cell cycle gene expression during quiescence.

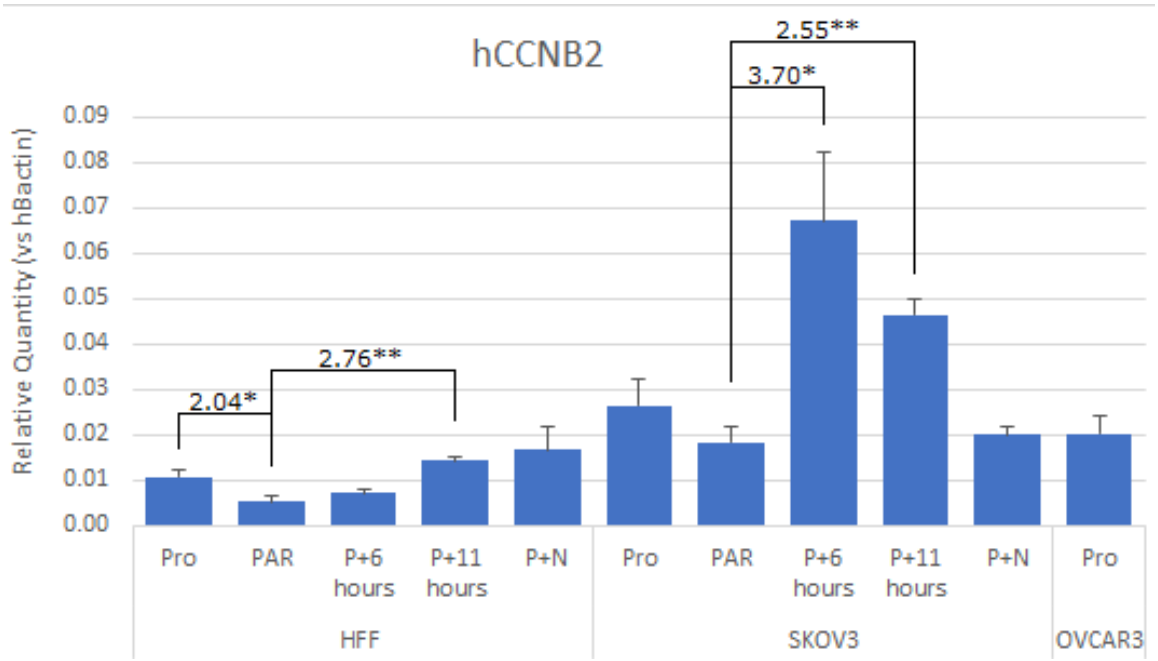

Figure 9: RT-qPCR gene expression analysis of the hCCNB2. Each treatment, proliferating, PAR (G0/G1), P+6 hours (late G1), P+11 hours (S phase), and P+N (G2), are shown from the left to right respectively for both HFF (left) and SKOV3 (right). Each cell cycle phase was compared to the cells arrested in the G0/G1, PAR condition for HFF and SKOV3 cells. * indicates <0.05 and ** indicates <0.01 p-value.

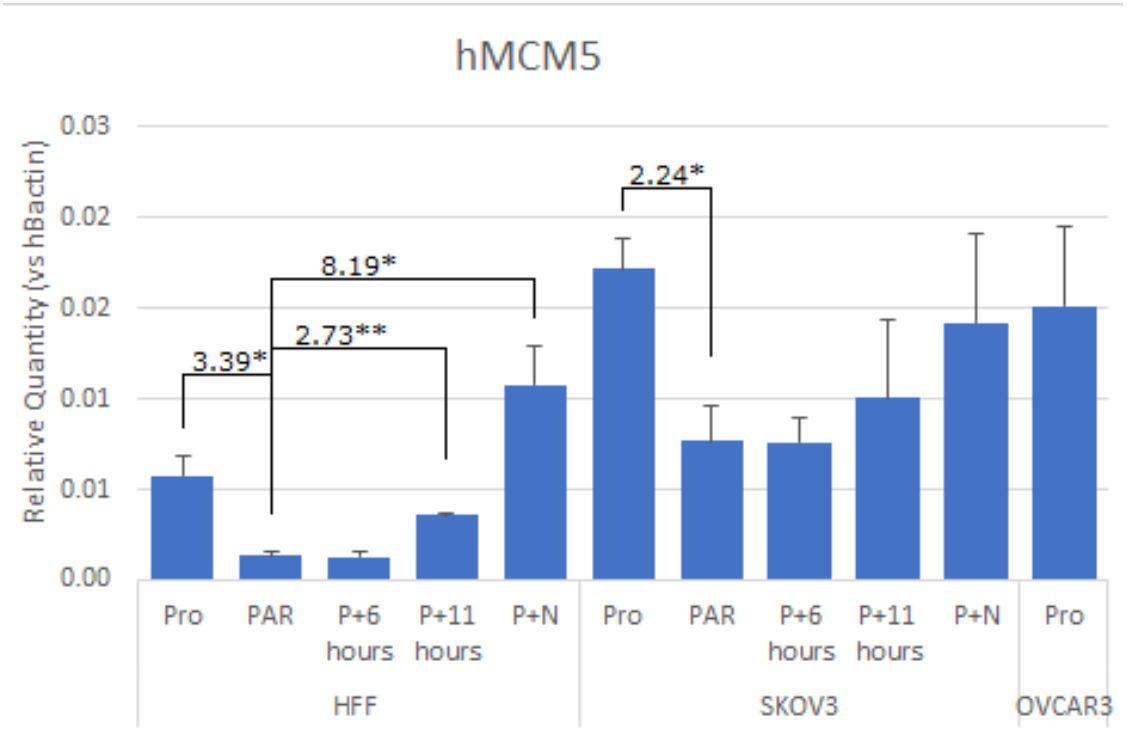

Figure 10: RT-qPCR gene expression analysis of the hCCNB2. Each treatment, proliferating, PAR (G0/G1), P+6 hours (late G1), P+11 hours (S phase), and P+N (G2), are shown from the left to right respectively for both HFF (left) and SKOV3 (right). Each cell cycle phase was compared to the cells arrested in the G0/G1, PAR condition for HFF and SKOV3 cells. * indicates <0.05 and ** indicates <0.01 p-value.

4 Discussion

Recurrent and metastatic cancer can be caused by cancer cells that were able to survive chemotherapy and radiation by entering quiescence.[54] pRb and p130 are both major regulators of quiescence in cells.[1] Despite understanding how these proteins work in normal cells, there was a gap in knowledge surrounding the presence and behavior of these proteins in cancerous cells. Using flow cytometry, we were able to characterize that the HFF cells and SKOV3 cancer cells both responded to CDK inhibition which be observed in Figures 3 and 4. CDK inhibition arrests cells in the G0/G1 state, suggesting these cells are entering quiescence. The OVCAR3 cells did not respond to the PAR drug treatment, as seen in Figure 5, and this result is consistent with previous findings that OVCAR3 cells do not respond to CDK inhibition.[50]

The Western blots revealed that OVCAR3 cells do not express p130 but do express pRb.[55] This observation indicates pRb is completely dysfunctional in the OVCAR3 cells, since they did not respond to CDK inhibition. Both pRb and p130 were present in the cell at each phase of the cell cycle in the HFF and SKOV3 cells. Further investigation showed that phosphorylated pRb was present in the SKOV3 PAR treated sample. This defied the expectation that the proteins would be unphosphorylated and active (Figure 7E). This result indicates that pRb is not completely unphosphorylated during quiescence, and cell cycle genes are expressed. Further investigation is needed to understand how partial phosphorylation of pRb affects the cell's abilities to stay quiescent. To accomplish this, modifications of the time course to focus on the behavior of pRb and p130 as the cells are entering quiescence in addition to the behavior of the proteins as they are phosphorylated after being released from the PAR treatment.

In the mRNA expression analysis, we saw significant differences in the expression of the hCCNB2 and hMCM5 genes in the SKOV3 cells compared to HFF control cells. In hCCNB2, there was a lack of repression of cell cycle gene in the PAR treated sample in the SKOV3 cells. Similarly, the hMCM5 gene had no significant fold change between the proliferating and the PAR sample in the SKOV3 cells. These results indicate that the genes are not being completely shut off during quiescence. We speculate that because pRb is partially phosphorylated during quiescence, as shown in the phosphorylated Western (Figure 7E), it is causing cell cycle genes to be transcribed in G0, which is seen in the hMCM5 and hCCNB2 genes. Further studies will need to be conducted to determine how this affects SKOV3 cells' ability to quiesce and evade cancer therapies.

Exhibiting behavior similar to brakes in a car, pRb and p130 bind to their E2F transcription factors to stop cell cycle progression. When pRb and p130 are not phosphorylated, they are active, and the brake is applied to the cell cycle. After receiving the external stimulation that the cell requires for division, the cyclin D: CDK 4/6 complex phosphorylates pRb and p130. This can be compared to removing the brake from the cell cycle. Mutations in pRb and p130 cause the brakes in cell division to malfunction. If the cell cycle cannot be suppressed, the cell will become cancerous. Understanding how pRb and p130 are behaving in cancerous cells will provide insight to enhance the efficacy of cancer treatments.

Overall, the behavior of pRb and p130 in quiescing cancer cells is still understudied. Looking forward, the best way to continue the characterization of the differences in quiescing and non-quiescing cancer cells is to compare them to

noncancerous cells with chromatin immunoprecipitation (ChIP) of pRb, p130, and their E2F binding partners. Moving forward, ChIP-seq would identify specifically where these proteins are binding to the DNA. Similarly, RNA-seq would characterize the genome-wide effects on cell cycle gene expression and regulation. Understanding the interactions between the genome, transcriptome, and the proteome and their effects on gene expression could reveal key information about the regulation of quiescence.

5 Conclusion

From the information we gathered, it is still unclear how pRb and p130 are affected in cancer cells that can quiesce. However, with the experiments that are in progress, we should gain more insight into how pRb and p130 are affected in cancer cells. We determined that pRb was completely dysfunctional in the OVCAR3 cells as the p130 protein was absent in that cell line. This explains why they were resistant to the PAR treatment. The Western blots confirmed that both pRb and p130 are present in both the HFF and SKOV3 cells at each phase of the cell cycle. The phosphorylated-Western blots showed the presence of phosphorylated pRb in the SKOV3 cells after they were treated for 24 hours with PAR. The PAR treatment should have inactivated the cyclin D: CDK4/6 complex that is responsible for phosphorylating pRb and p130. This observation indicates there is some dysfunction of the pRb protein in the SKOV3 cells. mRNA expression analysis of hCCNB2 and hMCM5 cell cycle genes showed that the SKOV3 cells have decreased fold changes between the proliferating and the PAR treated samples, which again indicates that pRb or p130 are partially deactivated in quiescence when they're supposed to be completely activated. Advancing the understanding of pRb and p130's function in the quiescent pathway in cancer cells is crucial to treating cancer patients more effectively. Because chemotherapies and radiation are anti-prolific treatments, they target the cells that are actively dividing. If cancer cells can enter quiescence, a non-proliferative state, they evade those cancer treatments. If pRb is malfunctioning in quiescent cancer cells, the DREAM complex could be allowing cancer cells to retain their quiescent function. Locking p130 into a phosphorylated state would permanently inactivate the protein, which would prevent the cell from being able to enter

quiescence, and it could increase the efficacy of chemotherapy and radiation treatments. The increase in cancer treatment efficacy would result in less recurrent and metastatic cancer caused by quiescent cancer cells in all types of cancer.

6 Reference List

1. Jungeun Sarah Kwon, N. J. E., Xia Wang, Weikang Wang, Kimiko Della Croce, Jianhua Xing, Guang Yao. Controlling Depth of Cellular Quiescence by an Rb-E2F Network Switch. Cell Reports 20, 12, doi: 10.1016/j.celrep.2017.09.007 (2017).
2. Nevins, J. R. Toward an understanding of the functional complexity of the E2F and retinoblastoma families. Cell Growth and Differentiation 9, 585-593 (1998).
3. Kristian Helin. Regulation of cell proliferation by the E2F transcription factors. Current Opinion in Genetics and Development 8, 28-35, doi:10.1016/S0959-437X(98)80058-0 (1998).
4. Dyson, N. The regulation of E2F by pRB-family proteins. Genes and Development 12, 2245-2262, doi:0.1101/gad.12.15.2245 (1998).
5. Larisa Litovchick, S. S., Laurence Florens, Xiaopeng Zhu, Selene K. Swanson, Soundarapandian Velmurugan, Runsheng Chen, Michael P. Washburn, X Shirley Liu, James A. DeCaprio. Evolutionarily Conserved Multisubunit RBL2/p130 and E2F4 Protein Complex Represses Human Cell Cycle-Dependent Genes in Quiescence. *Molecular Cell* **26**, 539-551, doi:10.1016/j.molcel.2007.04.015 (2007).
6. M Pilkinton, R. S., O R Colamonici. Mammalian Mip/LIN-9 interacts with either the p107, p130/E2F4 repressor complex or B-Myb in a cell cycle-phase-dependent context distinct from the Drosophila dREAM complex. *Oncogene* **26**, 7535-7543, doi:10.1038/sj.onc.1210562 (2007).
7. Subhashini Sadasivam, J. A. D. The DREAM complex: Master coordinator of cell cycle dependent gene expression. *Nature Reviews Cancer* **13**, 585-595, doi:10.1038/nrc3556 (2013).
8. Benjamin R. Topacio, E. Z., Sandra Cristea, Shicong Xie, Carrie S. Tambo, Seth M. Rubin, Julien Sage, Mardo Kõivomägi, and Jan M. Skotheim. Cyclin D-Cdk4,6 Drives Cell-Cycle Progression via the Retinoblastoma Protein's C-Terminal Helix. *Molecular Cell* **74**, doi:10.1016/j.molcel.2019.03.020. (2019).
9. Anil M Narasimha, M. K., Gary S Shapiro, Yoon J Choi, Piotr Sicinski, Steven F Dowdy. Cyclin D activates the Rb tumor suppressor by mono-phosphorylation. eLife 3, doi:10.7554/eLife.02872 (2014).
10. Hilary A Coller, L. S., James M Roberts. A New Description of Cellular Quiescence. *Plos Biology* **4**, doi:10.1371/journal.pbio.0040083 (2006).
11. O'Farrell, P. H. Quiescence: early evolutionary origins and universality do not imply uniformity. The Royal Society 366, 3498–3507, doi:10.1098/rstb.2011.0079 (2011).
12. Nik Nabil, W. N. et al. Towards a Framework for Better Understanding of Quiescent Cancer Cells. Cells 10, doi:10.3390/cells10030562 (2021).
13. Nor Rashid, N., Yusof, R. & Watson, R. J. Disruption of repressive p130–DREAM complexes by human papillomavirus 16 E6/E7 oncoproteins is required for cell-cycle progression in cervical cancer cells. *Journal of General Virology* **92**, 2620-2627, doi:10.1099/vir.0.035352-0 (2011).

14. C Giacinti, A. G. RB and Cell Cycle Progression. Oncogene 25, 5220-5227, doi:10.1038/sj.onc.1209615 (2006).
15. Vermeulen, K., Van Bockstaele, D. R. & Berneman, Z. N. The cell cycle: a review of regulation, deregulation and therapeutic targets in cancer. Cell Proliferation 36, 131-149, doi:10.1046/j.1365-2184.2003.00266.x (2003).
16. Sabrina L Spencer, S. D. C., Feng-Chiao Tsai, K Wesley Overton, Clifford L Wang, Tobias Meyer. The proliferation-quiescence decision is controlled by a bifurcation in CDK2 activity at mitotic exit. *Cell* **155**, 369-383, doi:10.1016/j.cell.2013.08.062 (2013)
17. Tyson, J. J., Csikasz-Nagy, A. & Novak, B. The dynamics of cell cycle regulation. Bioessays 24, 1095-1109, doi:10.1002/bies.10191 (2002).
18. Tom H. Cheung and Thomas A. Rando. Molecular regulation of stem cell quiescence. Nature Reviews Molecular Cell Biology 14, 329-340, doi:10.1038/nrm3591 (2013).
19. Jedrzejczak-Silicka, M. History of Cell Culture. IntechOpen, doi:10.5772/66905 (2016).
20. Krafts, K. P. Tissue Repair. Organogenesis 6, 225-233, doi:10.4161/org.6.4.12555 (2010).
21. Christiana M. Neophytou, T.-C. K., Panagiotis Papageorgis. Mechanisms of Metastatic Tumor Dormancy and Implications for Cancer Therapy. International Journal of Molecular Sciences 20, doi:10.3390/ijms2024615518 (2019).
22. Amy E. Schade, M. G. O., Hilary E. Nicholson, James A. DeCaprio. Cyclin D–CDK4 relieves cooperative repression of proliferation and cell cycle gene expression by DREAM and RB. *Oncogene* **38**, 4962-4976, doi:10.1038/s41388-019-0767-9 (2019).
23. Y Takahashi, J. B. R., B D Dynlacht. Analysis of promoter binding by the E2F and pRB families in vivo: distinct E2F proteins mediate activation and repression. *Genes and Development* **14**, 804-816 (2000).
24. Amy E Schade, M. F., James A DeCaprio. RB, p130 and p107 differentially repress G1/S and G2/M genes after p53 activation. *Nucleic Acids Research* **47**, 11197-11208, doi:10.1093/nar/gkz961 (2019).
25. Stacey E Wirt, J. S. p107 in the public eye: an Rb understudy and more. *Cell Division* **5**, doi:Wirt SE, Sage J. p107 in the public eye: an Rb understudy and more. Cell Div. 2010;5:9. Published 2010 Apr 2. doi:10.1186/1747-1028-5-9 (2010).
26. Marco Gründl, S. W., Laura Hauf, Melissa Schwab, Kerstin Marcela Werner, Susanne Spahr, Clemens Schulte, Hans Michael Maric, Carsten P. Ade, Stefan Gaubatz. Interaction of YAP with the Myb-MuvB (MMB) complex defines a transcriptional program to promote the proliferation of cardiomyocytes. *PLOS Genetics* **16**, doi:10.1371/journal.pgen.1008818 (2020).
27. MarieClasson, N. p107 and p130: Versatile Proteins with Interesting Pockets. Experimental Cell Research 261, 135-147, doi:10.1006/excr.2000.5135 (2001).
28. Douglas Hanahan, R. A. The Hallmarks of Cancer. Cell 100, doi:10.1016/S0092-8674(00)81683-9 (2000).

29. Thomas C. Lee, D. S. G., J. William Harbour, Nancy C. Mansfield, A. Linn Murphree. Retina. 5th edn, Vol.3 2104-2149 (W. B. Saunders, 2013).
30. SibylleMittnacht. The retinoblastoma protein—from bench to bedside. European Journal of Cell Biology 84, 97-107, doi:10.1016/j.ejcb.2004.12.012 (2005).
31. E K Flemington, S. H. S., W G Kaelin Jr. E2F-1-mediated transactivation is inhibited by complex formation with the retinoblastoma susceptibility gene product. Proc. Natl. Acad. Sci. U. S. A. 90, 6914-6918, doi:10.1073/pnas.90.15.6914 (1993).
32. Helin, K., Harlow, E. & Fattaey, A. Inhibition of E2F-1 transactivation by direct binding of the retinoblastoma protein. Molecular and Cellular Biology 13, 6501-6508, doi:10.1128/mcb.13.10.6501-6508.1993 (1993).
33. Keelan Z. Guiley, T. J. L., Jessica G. Felthousen, Parameshwaran Ramanan, Larisa Litovchick, Seth M. Rubin. Structural mechanisms of DREAM complex assembly and regulation. Genes and Development 29, 9671-9974, doi:10.1101/gad.257568.114 (2015).
34. Nevins, J. R. E2F: a Link Between the Rb Tumor Suppressor Protein and Viral Oncoproteins. Science 258, 424-429, doi:10.1126/science.1411535 (1992).
35. Andrew W. Murray, M. J. S. M. W. K. The role of cyclin synthesis and degradation in the control of maturation promoting factor activity. *Nature* **339**, 280-286, doi:10.1038/339280a0 (1989).
36. Siegel, R. L., Miller, K. D., Fuchs, H. E. & Jemal, A. Cancer Statistics, 2021. CA: A Cancer Journal for Clinicians 71, 7-33, doi:10.3322/caac.21654 (2021).
37. Torre, L. A. et al. Ovarian cancer statistics, 2018. CA: A Cancer Journal for Clinicians 68, 284-296, doi:10.3322/caac.21456 (2018).
38. Chávarri-Guerra, Y., González-Ochoa, E., De-la-Mora-Molina, H. & Soto-Perez-de-Celis, E. Systemic therapy for non-serous ovarian carcinoma. Chin Clin Oncol 9, 52, doi:10.21037/cco-20-36 (2020).
39. Amelia Hallas-Potts, J. C. D., C. Simon Herrington. Ovarian cancer cell lines derived from non-serous carcinomas migrate and invade more aggressively than those derived from high-grade serous carcinomas. Scientific Reports 9, doi:10.1038/s41598-019-41941-4 (2019).
40. Michael-Antony Lisio, L. F., Alicia Goyeneche, Zu-hua Gao, and Carlos Telleria. High-Grade Serous Ovarian Cancer: Basic Sciences, Clinical and Therapeutic Standpoints. International Journal of Molecular Sciences 20, doi:10.3390/ijms20040952 (2019).
41. Wilson, M. A. J. a. L. Microtubules as a target for anticancer drugs. Nature Reviews Cancer 4, 253–265, doi:10.1038/nrc1317 (2004).
42. Perez, E. A. Microtubule inhibitors: Differentiating tubulin-inhibiting agents based on mechanisms of action, clinical activity, and resistance. Molecular Cancer Therapeutics 8, 2086-2095, doi:10.1158/1535-7163.Mct-09-0366 (2009).
43. Mukhtar, E., Adhami, V. M. & Mukhtar, H. Targeting Microtubules by Natural Agents for Cancer Therapy. Molecular Cancer Therapeutics 13, 275-284, doi:10.1158/1535-7163.Mct-13-0791 (2014).

44. Wanting Chen, J. D., Jacques Haiech, Marie-Claude Kilhoffer, and Maria Zeniou. Cancer Stem Cell Quiescence and Plasticity as Major Challenges in Cancer Therapy. Stem Cells International 2016, 16, doi:10.1155/2016/1740936 (2016).
45. Lin, S.-h. W. a. S.-Y. Tumor dormancy: potential therapeutic target in tumor recurrence and metastasis prevention. Experimental Hematology and Oncology 2, doi:10.1186/2162-3619-2-29 (2013).
46. María Soledad Sosa, P. B. J. A. A.-G. Mechanisms of disseminated cancer cell dormancy: an awakening field. Nature Reviews Cancer 14, 611-622, doi:10.1038/nrc3793 (2014).
47. Richard S Finn, J. D., Dylan Conklin, Ondrej Kalous, David J Cohen, Amrita J Desai, Charles Ginther, Mohammad Atefi, Isan Chen, Camilla Fowst, Gerret Los, Dennis J Slamon. PD 0332991, a selective cyclin D kinase 4/6 inhibitor, preferentially inhibits proliferation of luminal estrogen receptor-positive human breast cancer cell lines in vitro. *Breast Cancer Res* **11**, doi:https://doi.org/10.1186/bcr2419 (2009).
48. Gottfried E Konecny, B. W., Teodora Kolarova, Jingwei Qi, Kanthinh Manivong, Judy Dering, Guorong Yang, Meenal Chalukya, He-Jing Wang, Lee Anderson, Kimberly R Kalli, Richard S Finn, Charles Ginther, Siân Jones, Victor E Velculescu, Darren Riehle, William A Cliby, Sophia Randolph, Maria Koehler, Lynn C Hartmann, Dennis J Slamon. Expression of p16 and retinoblastoma determines response to CDK4/6 inhibition in ovarian cancer. *Clinical Cancer Research* **17**, 11, doi:10.1158/1078-0432.CCR-10-2307 (2011).
49. Alessandra Dall'Acqua, M. B., Nastaran Masoudi-Khoram, Roberto Sorio, Fabio Puglisi, Barbara Belletti, and Gustavo Baldassarre. Inhibition of CDK4/6 as Therapeutic Approach for Ovarian Cancer Patients: Current Evidences and Future Perspectives. *Cancers* **13**, doi:10.3390/cancers13123035 (2021).
50. Barbie Taylor-Harding, P.-J. A., Hasmik Agadjanian, Dong-Joo Cheon, Takako Mizuno, Danielle Greenberg, Jenieke R. Allen, Lindsay Spurka, Vincent Funari, Elizabeth Spiteri, Qiang Wang, Sandra Orsulic, Christine Walsh, Beth Y. Karlan, and W. Ruprecht Wiedemeyer. Cyclin E1 and RTK/RAS signaling drive CDK inhibitor resistance via activation of E2F and ETS. *Oncotarget* **6**, 18, doi:10.18632/oncotarget.2673 (2014).
51. Hagan, E. W. T. a. I. M. Release from cell cycle arrest with Cdk4/6 inhibitors generates highly synchronized cell cycle progression in human cell culture. *Open Biology* **10**, 18, doi:10.1098/rsob.200200 (2020).
52. Christina FS Mages, A. W., Stephan H Bernhart, and Gerd A Müller. The DREAM complex through its subunit Lin37 cooperates with Rb to initiate quiescence. eLife 8, doi:10.7554/eLife.26876 (2017).
53. Ting Wu, X. Z., Xiaohua Huang, Yuqing Yang, and Xianxin Hua. Regulation of Cyclin B2 Expression and Cell Cycle G2/M Transition by Menin. *Journal of Biological Chemistry* **285**, 9, doi:10.1074/jbc.M110.106575 (2010).
54. Nam, S.-Y. P. J.-S. The force awakens: metastatic dormant cancer cells. *Experimental & Molecular Medicine* **52**, 12, doi:10.1038/s12276-020-0423-z (2020).

55. Y Yaginuma, H. H., K Kawai, T Kurakane, Y Saitoh, S Kitamura, K Sengoku, M Ishikawa. Analysis of the Rb gene and cyclin-dependent kinase 4 inhibitor genes (p16INK4 and p15INK4B) in human ovarian carcinoma cell lines. *experimental Cell Research* **233**, 7, doi:10.1006/excr.1997.3560 (1997).